PCT WORLD INTELLECTUAL PROPEI
International Bu

INTERNATIONAL APPLICATION PUBLISHED UNDER WO 9608835A1

(51) International Patent Classification 6 :
H01J 37/29, 37/244

A1

(11) International Publication Number: **WO 96/08835**

(43) International Publication Date: 21 March 1996 (21.03.96)

(21) International Application Number: PCT/US95/10566

(22) International Filing Date: 17 August 1995 (17.08.95)

(30) Priority Data:
08/305,382 13 September 1994 (13.09.94) US

(71) Applicant *(for all designated States except US)*: METROLOGIX, INC. [US/US]; 2367 Bering Drive, San Jose, CA 95131 (US).

(72) Inventor; and
(75) Inventor/Applicant *(for US only)*: MONAHAN, Kevin, M. [US/US]; 11877 Woodhill Court, Cupertino, CA 95014 (US).

(74) Agent: KREBS, Robert, E.; Burns, Doane, Swecker & Mathis, P.O. Box 1404, Alexandria, VA 22313-1404 (US).

(81) Designated States: CA, CN, JP, KR, SG, US, European patent (AT, BE, CH, DE, DK, ES, FR, GB, GR, IE, IT, LU, MC, NL, PT, SE).

Published
With international search report.

(54) Title: PARTICLE BEAM DETECTOR PROVIDING Z-AXIS AND TOPOGRAPHIC CONTRAST

(57) Abstract

The present invention, generally speaking, using various detector configurations, provides improved imaging techniques for high resolution inspection and precision measurement of sub-micron features. The detector configurations provide z-axis contrast (sensitivity to upper and lower surfaces), topographic contrast (sensitivity to rising and falling edges), or both. In particular, an inspection and measurement apparatus of the present invention includes a stage for supporting a wafer on which a microscopic structure is formed, an arrangement for directing a primary electron beam onto the microscopic structure, and multiple detectors spaced apart substantially different scalar distances from one of: a) in the horizontal direction, a primary electron-optical axis (47); and b) in the vertical direction, a wafer plane (43). Detectors (A, B, C, D) spaced apart in the horizontal direction provide topographical contrast, whereas detectors (LD, UD) spaced apart in the vertical direction provide Z-axis contrast.

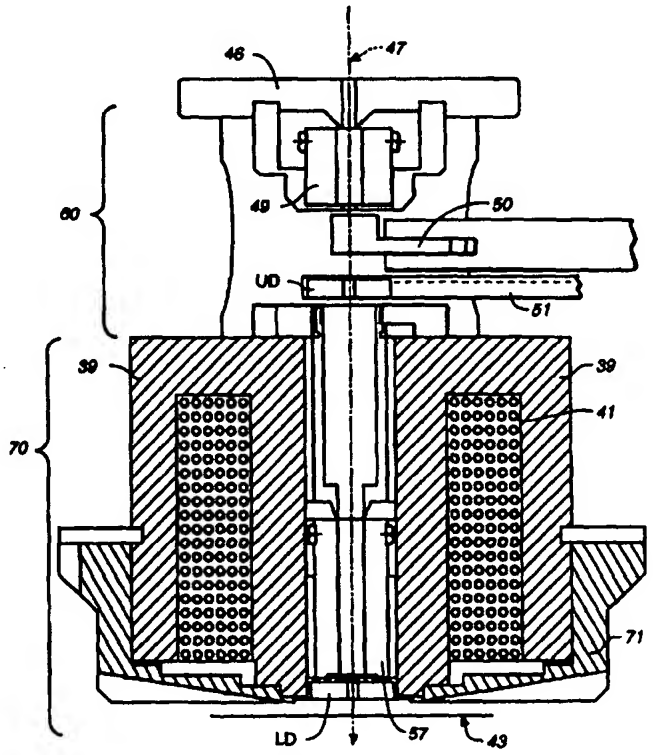

FOR THE PURPOSES OF INFORMATION ONLY

Codes used to identify States party to the PCT on the front pages of pamphlets publishing international applications under the PCT.

AT	Austria	**GB**	United Kingdom	**MR**	Mauritania
AU	Australia	**GE**	Georgia	**MW**	Malawi
BB	Barbados	**GN**	Guinea	**NE**	Niger
BE	Belgium	**GR**	Greece	**NL**	Netherlands
BF	Burkina Faso	**HU**	Hungary	**NO**	Norway
BG	Bulgaria	**IE**	Ireland	**NZ**	New Zealand
BJ	Benin	**IT**	Italy	**PL**	Poland
BR	Brazil	**JP**	Japan	**PT**	Portugal
BY	Belarus	**KE**	Kenya	**RO**	Romania
CA	Canada	**KG**	Kyrgystan	**RU**	Russian Federation
CF	Central African Republic	**KP**	Democratic People's Republic of Korea	**SD**	Sudan
CG	Congo			**SE**	Sweden
CH	Switzerland	**KR**	Republic of Korea	**SI**	Slovenia
CI	Côte d'Ivoire	**KZ**	Kazakhstan	**SK**	Slovakia
CM	Cameroon	**LI**	Liechtenstein	**SN**	Senegal
CN	China	**LK**	Sri Lanka	**TD**	Chad
CS	Czechoslovakia	**LU**	Luxembourg	**TG**	Togo
CZ	Czech Republic	**LV**	Latvia	**TJ**	Tajikistan
DE	Germany	**MC**	Monaco	**TT**	Trinidad and Tobago
DK	Denmark	**MD**	Republic of Moldova	**UA**	Ukraine
ES	Spain	**MG**	Madagascar	**US**	United States of America
FI	Finland	**ML**	Mali	**UZ**	Uzbekistan
FR	France	**MN**	Mongolia	**VN**	Viet Nam
GA	Gabon				

PARTICLE BEAM DETECTOR PROVIDING Z-AXIS AND TOPOGRAPHIC CONTRAST

BACKGROUND OF THE INVENTION

Field of the Invention

The present invention relates to particle beam metrology wherein a particle beam device such as a scanning electron microscope is used to inspect and perform critical dimension measurements of objects, for example integrated circuit wafers.

State of the Art

It is known to use electromagnetic systems in microscopes such as scanning electron microscopes (SEM) for inspection and measurement purposes. Scanning electron microscopes are often used in place of traditional optical microscopes for microelectronics inspection and metrology applications in semiconductor manufacturing. The metrology tools are often used, for example, for measuring patterns (i.e. critical dimensions) formed on semiconductor wafers during fabrication.

The short wavelengths of scanning electron microscopes have several advantages over conventionally used optical microscopes. For example, scanning electron microscopes can achieve resolutions from about 25Å to 100Å, while the limit of resolution of optical microscopes is typically about 2500Å. Further, scanning electron microscopes provide depth of field greater than optical microscopes. Despite the accuracy and precision of present scanning electron microscopes, enhanced instrument specifications and capabilities are

required as parameters (e.g. critical dimensions) to be inspected come within the sub-micrometer range.

An article entitled "Microelectronics Dimensional Metrology in the Scanning Electron Microscope", Parts I and II, Solid State Technology, by Michael T. Postek et al. (November 1986), describes a typical SEM wafer inspection system. As described therein, as focused electron beam is scanned from point to point on the specimen surface in a rectangular raster pattern. Accelerating voltage, beam current and spot diameter are optimized for the specific application and specimen composition.

As the scanning electron beam contacts the surface of the specimen, backscattered and/or secondary electrons are emitted from the specimen surface. Semiconductor inspection, analysis and metrology is performed by detecting the backscattered and/or secondary electrons. A point by point representation of the specimen is obtained on a CRT screen as the electron beam controllably scans the specimen.

Conventionally, a particle beam device such as a scanning electron microscope 7, shown in Figure 1, includes a voltage source 11. The voltage source 11 is connected to an electron source 13 that directs a narrow beam of highly accelerated electrons towards a specimen stage 18 via a plurality of electron lenses L_1, L_2, and L_3. The electron beam is indicated by the dashed line 14. The electron beam may be focused onto a wafer stage of the scanning electron microscope using an autofocus technique.

As further shown in Figure 1, a cylindrical column 17 houses the electron source 13 and the lenses L_1, L_2, and L_3. The column 17 is normally referred to as an electron optical column and includes a chamber, indicated in the drawing as 17A, that surrounds and supports a specimen stage 18.

Together, the optical column 17 and the chamber 17A represent the body of the scanning electron microscope.

The scanning electron microscope 7 of Figure 1 further includes an electromagnetic or electrostatic deflection system for selectively scanning the electron beam across the specimen stage 18. The deflection system shown includes four pairs of electron beam scanning coils, designated D_1 through D_4. The scanning coils are located within optical column 17 for focusing the electron beam on the surface of the specimen held on stage 18. The pair of deflection coils D_1 and D_2 are connected to sawtooth voltage generator 19, and the pair of deflection coils D_3 and D_4 are connected to sawtooth voltage generator 20.

The electron beam scanning coils D_1 through D_4 deflect the electron beam 14 in two, generally perpendicular, directions. In the drawing, the deflection directions are designated as the x-direction and the y-direction, respectively. The x-direction and the y-direction typically are in a plane perpendicular to the direction of beam 14, but strict orthogonality is not required. For present purposes, it can be assumed that coils D_1 and D_3 deflect the scanning beam in the x-direction and that coils D_2 and D_4 deflect the scanning beam in the y-direction.

An electron collector 22 is arranged near the surface of a stage 18 which is exposed to beam 14. The electron collector is connected to an amplifier 23 which provides signals to an analog-to-digital converter 43 for transforming the collected electron current to digital signals which may be subsequently displayed on a video display 49.

In operation, saw-tooth generators 19 and 20 provide time-varying voltage signals to electron beam scanning coils D_1 and D_4 such that beam 14 is deflected across specimen stage 18 in a predetermined scanning pattern. The

saw-tooth generators 19 and 20 typically operate synchronously to drive the electron beam across stage 18 in the x-direction at a constant rate, with each scan beam deflected in the y-direction to form a series of generally parallel scanning lines.

During operation of the Figure 1 scanning electron microscope, collector 22 detects changes in the electron current at stage 18. Thus, as the electron beams scans a specimen on stage 18, changes in the composition, texture and topography of the specimen causing amplitude variations of the electron current detected by collector 22. With each complete scanning sequence, an image corresponding to features of the specimen can be created.

Traditional methods of electron imaging rely on secondary electron emission and, as a result, have limited capability for extracting information from the base of sub-micrometer contact holes and other high-aspect-ratio structures. Such a high-aspect-ratio contact hole is a common feature of semiconductor wafers and is shown in Figure 2. A layer of resist 31 has been used to pattern a sub-micrometer contact hole in a layer of oxide 33 coated on the surface of a wafer 35. The height h of the contact hole is considerably greater than the width w of the contact hole such that $h/w >> 1$. Typical values of h and w might be 2.0μm and 0.5μm respectively, giving an aspect ratio of 4:1.

The difficulty of imaging high-aspect-ratio structures using traditional methods of secondary electron imaging holds particularly true for structures with nearly vertical profiles. Because of the insulating properties of oxide and photoresist, directing a primary electron beam onto the wafer structure causes negative surface charge to accumulate at the surface of the photoresist layer as illustrated at Figure 3. A few volts of surface potential can severely disturb the secondary electron image, since secondary electrons (SE) are typically emitted with energies less than 10 electron volts. In cases of severe charging,

commonly encountered when imaging contact holes, secondary electron emission from the base may be shut off entirely, leaving only the signal from backscattered electrons (BSE). Attempts to control surface fields have been only partially effective and may themselves introduce artifacts by modulating the landing energy of the primary electron beam.

The inability of conventional secondary and backscattered (BSE) electron imaging techniques to effectively image high-aspect-ratio structures is further exacerbated by the situation such as illustrated in Figure 4. The current art teaches that, for greatest collector efficiency, an electron detector 37 must be placed so that its effective *cone of vision, or acceptance angle,* barely penetrates inside the contact hole. The bottom of the contact hole, which is of greatest interest to assure that penetration of the oxide layer has occurred, cannot even be imaged. This result is seen clearly in Figure 5, showing a scanning electron micrograph using traditional methods of 0.5μm contact holes in a 2.0μm layer of photoresist and oxide. The regions in the vicinity of the contact openings appear as darkened circles. The darkened circles, however, rather than conveying information concerning the base of the contact holes, convey a lack of information thereof.

Accordingly, a need exists for improved imaging techniques for extracting information from the base of sub-micrometer contact holes and other high-aspect-ratio structures. A need also exists for imaging techniques providing improved sensitivity to rising and falling edges. Sensitivity to rising and falling edges may be termed "topographic contrast", whereas sensitivity to upper and lower surfaces may be formed "Z-axis contrast".

SUMMARY OF THE INVENTION

The present invention, generally speaking, using various detector configurations, provides improved imaging techniques for high resolution

inspection and precision measurement of sub-micron features. The detector configurati ns provide Z-axis contrast (sensitivity to upper and lower surfaces) topographic contrast (sensitivity to rising and falling edges), or both.

In particular, an inspection and measurement apparatus of the present invention includes a stage for supporting a wafer on which a microscopic structure is formed, an arrangement for directing a primary electron beam onto the microscopic structure, and multiple detectors spaced apart substantially different scalar distances from one of: a) in the horizontal direction, a primary electron-optical axis; and b) in the vertical direction, a wafer plane. Detectors spaced apart in the horizontal direction provide topographical contrast, whereas detectors spaced apart in the vertical direction provide Z-axis contrast.

BRIEF DESCRIPTION OF THE DRAWINGS

The invention may be further understood from the following written description in conjunction with the appended drawings. In the drawings:

Figure 1 is a simplified diagram of a conventional scanning electron microscope;

Figure 2 is a sectional view of a contact hole portion of a semiconductor wafer structure;

Figure 3 is a sectional view, like that of Figure 2, showing the effects of surface charge accumulation;

Figure 4 is a sectional view showing the limited penetration into a high-aspect-ratio structure of the cone of vision of an electron detector;

Figure 5 is a scanning electron micrograph using traditional techniques of high-aspect-ratio contact holes;

Figure 6 is a corresponding scanning electron micrograph using the techniques of the present invention;

Figure 7 is a diagram representing the operation of two signal detection sub-systems in accordance with the present invention;

Figure 8 is a corresponding diagram illustrating a negative-bias electron discrimination technique;

Figure 9 is a diagram showing the opposite effect on upper and lower detector signals as a high-aspect-ratio contact hole is scanned;

Figure 10 is a diagram showing a negative electron optical working distance used in conjunction with the present invention;

Figure 11 is a sectional view of an optical column in accordance with an embodiment of the present invention;

Figure 12 is a sectional view showing in greater detail features of the electron optics of an embodiment of the present invention;

Figure 13 is a block diagram of circuitry for combining signals from the upper and lower detectors;

Figure 14 is a diagram representing detection of secondary electrons at an upper detection in accordance with an alternate embodiment of the invention;

Figure 15A is a diagram of a detector arrangement affording topographic contrast;

Figure 15B is a plan view of a quad detector arrangement that may be used to provide topographic contrast in two topographic directions;

Figure 16 is a diagram of a detector arrangement that affords both topographic and Z-axis contrast;

Figure 17 is a plan view of a detector configuration in which two concentric annular detectors provide Z-axis contrast only;

Figure 18 is a plan view of a detector arrangement in which two concentric annular quad detectors provide both topographic and Z-axis contrast; and

Figure 19 is a computer simulation of trajectories of elastically backscattered electrons through the electron microscope column of Figure 12.

DETAILED DESCRIPTION OF THE PREFERRED EMBODIMENTS

Prior attempted solutions to the problem of imaging high-aspect-ratio structures have attempted to improve the signals-to-noise ratio of the detected signal by improving secondary electron collection efficiency. Secondary electron yields, however, are already high, approaching unity, therefore leaving little room for improvement. The techniques to be presently described take an opposite approach by concentrating instead on backscattered electrons (BSE) whose yield is much lower than that of secondary electrons. Backscatter yields are typically on the order of 10%. Despite their lower emission yields, however, backscattered electrons exhibit a much higher energy (nearly equal to the energy of the primary scanning electron beam, approximately 1000eV) than

secondary electrons (less than 10eV). The high-energy backscattered electrons are extremely resistant to charge on the surface of the sample, as shown in Figure 3, and therefore produce better images in regions of holes and trenches despite their lower emission yields.

Referring to Figure 7, high-aspect-ratio structures such as microelectronic contact holes may be imaged using two signal detection subsystems, one optimized for imaging at the top and another optimized for imaging at the base of sub-micrometer structures. In a preferred embodiment, both detectors are of a microchannel plate detectors of a type well-known in the art. Hereinafter, the detector furthest removed from the object being imaged will be referred to as the upper detector (UD), and the detector closest to the object being imaged will be referred to as the lower detector (LD). As seen in Figure 7, the imaging geometry associated with the lower detector is best adapted for imaging the top surface of the object, and the imaging geometry associated with the upper detector is best adapted for imaging at the base of troughs and holes. In particular, the lower detector receives backscatter emission of electrons in a solid angle defined by θ_1, θ_2 where θ_1 is near 90° from the normal to the sample and θ_2 is near 45° from the normal, so that the resulting signal is dominated by electrons from the top surface. The upper detector receives backscatter electrons in a solid angle described by θ_3, θ_4 where θ_3 is less than 45° and θ_4 is near 0°, so that the resulting signal is dominated by electrons from holes and trenches. As described hereinafter, a magnetic field-immersion objective lens may be used to accomplish adjustment of θ_1, θ_2, θ_3 and θ_4. The geometry of Figure 7 accomplishes a spatial filtering whereby backscattered electrons and secondary emission electrons are discriminated from one another and imaged on the upper and lower detectors, respectively, to achieve top and base biased imaging. In a preferred embodiment, the lower detector is positioned inside an immersion electromagnetic lens, and the upper detector is positioned above the immersion electromagnetic lens.

Referring to Figure 8, the spatial filtering effect of the geometry illustrated in Figure 7 may be augmented by energy filtering to prevent secondary electrons from being imaged on the upper detector. In a preferred embodiment, the face of the upper detector is negatively biased (for example, to about -300 volts) so as to repel the low-energy back scattered and secondary electrons. The high-energy backscattered electrons, on the other hand, remain substantially unaffected by the negative bias.

As a result of the spatial filtering and the energy filtering means illustrated in Figures 7 and 8, the signal from the lower detector is at a near-zero minimum when the base of the structure is being scanned, whereas the signal from the upper detector exhibits its maximum at the base of the structure, allowing high-precision measurement with no need for extrapolation. Assume that the primary electron beam is scanned across the cross-section shown in Figure 9 in a left to right direction. As the top surface of the structure is being scanned, an abundance of electrons are emitted so as to strike the lower detector and produce a high level signal. Surface charge effects do not appreciably influence the signal. As the primary electron beam reaches the contact hole, however, the influence of surface charge effects increases. At the same time, fewer and fewer electrons reach the lower detector as a consequence of the lower detector imaging geometry. At the base of the hole, the signal from the lower detector therefore falls to a near-zero minimum. As the contact hole is passed over and the primary electron beam again lands on the upper surface of the structure, the signal from the lower detector again rises to a high level.

The signal from the upper detector exhibits exactly the opposite behavior. Backscattered electron yield increases with the atomic number of the material on which the primary electron beams lands. Photoresist compositions in general have a relatively low atomic number, whereas silicon has a relatively high atomic number. As the surface of the structure is being scanned,

relatively few backscattered electrons are produced. As the primary electron beam scans the bottom of the contact hole, large numbers of backscattered electrons are produced because of the high atomic number of silicon. As the primary electron beam passes over the contact hole and again lands on the upper surface of the structure, the number of backscattered electrons produced again decreases. The resulting image contrast is the reverse of that obtained from secondary electrons. This reverse image contrast is further assisted by the small acceptance angle of the upper detector, which reduces the unwanted signal from laterally scattered electrons emitted at the top surface of the structure.

The fact that the BSE signal is approximately proportional to the atomic number of the material is dramatically different as compared to the SE signal. The SE signal varies with surface topography, depends very heavily on the incident beam energy and current, and is sensitive to surface changing.

The correspondence between the scan signals produced by the lower and upper detectors in Figure 9 and the corresponding images shown in Figure 5 (lower detector) and Figure 6 (upper detector) may be readily appreciated. In relation to Figure 5, the signal from the lower detector drops to almost zero inside the contact hole, obscuring whatever information might otherwise have been extracted concerning the size and shape of the contact hole. In relation to Figure 6, the signal from the upper detector reaches a peak level when the primary electron beam is inside the contact hole. The size and shape of the contact hole are therefore clearly shown.

Collection efficiency of backscattered electrons may be further increased by providing a negative electron optical working distance for the scanning electron microscope. Referring to Figure 10, an electromagnetic immersion objective of the scanning electron microscope is principally composed of a toroidal, channel-shaped magnetic polepiece 39 and an electric winding 41

wound inside the channel of the polepiece. The electromagnetic immersion lens produces a magnetic flux pattern as shown. Conventionally, the magnetic flux pattern is precisely controlled in such a way as to compensate for aberrations. In conventional scanning electron microscopes, however, the electron-optical working distance is typically positive. The electron-optical working distance refers to the distance between the surface plane of the wafer (43) and a plane corresponding to a region of maximum flux density (45). In a preferred embodiment, this distance is slightly negative (approximately -1mm). In other words, the plane of the wafer surface (43) is positioned above a plane (45) corresponding to a region of maximum flux density. The effect of this slightly negative electron-optical working distance is to sweep backscattered electrons onto the channel plates of the upper and lower detectors. In particular, a negative electron optical working distance causes backscattered electrons to strike the detectors even when the electrons are emitted at a significant angle from normal. Since backscattered electrons are low-yield, the resulting increase in collection efficiency is of considerable significance.

Figure 11 shows in detail the electron column of a scanning electron microscope according to a preferred embodiment of the present invention. The electron beam path is represented by a vertical broken line 47 and extends down to the wafer plane 43. An upper electrostatic octupole assembly 49 functions to position the electron beam. An upper detector assembly 51 houses the upper detector, preferably a microchannel plate detector. A magnetic lens liner 55 is a tellurium copper shield that protects the beam from disturbances that might otherwise be created by eight teflon-coated wires use to control the octupole. It also holds the octupole in place. A lower electrostatic octupole assembly 57 functions to scan the electron beam back and forth across the surface of the wafer. The lower detector opposes the wafer surface and is preferably a microchannel plate detector.

Figure 12 shows the complete electron optics of a scanning electron microscope according to a preferred embodiment of the invention. An upper column assembly 60 houses the upper octupole, the spray aperture assembly 50 and the upper detector assembly 51 and includes an electron gun interface 46. A magnetic lens assembly 70 includes a magnetic lens pole-piece 39 and electric winding 41. Attached to the polepiece is a lens cap 71. The magnetic lens liner extends inside the magnetic lens assembly 70. Also housed inside the magnetic lens assembly 70 are the lower octupole assembly 57 and the lower detector.

The signals from the upper and lower detectors need not be used in exclusion to one another. Referring to Figure 13, preferably, the signals from the upper and lower detectors are combined in a variable ratio in accordance with a control arrangement to produce an image resembling an "extended focus" image. The signals may be combined in real time to produce a mixed-signal image having the inherent linearity and resolution characteristic of electron-beam technology. In particular, signals from the upper and lower detectors are input to variable-gain amplifiers 81 and 83, respectively. The gains of the amplifiers are set in accordance with control signals from a control unit 85. The output signals from the amplifiers are then summed in a summer 87, the output of which is sent to the CRT display.

In order to use backscattered electrons as the primary imaging mechanism for high aspect ratio structures, instead of the more widely used secondary electrons, a high beam current is required (because of the low yield of backscattered electrons). When inspecting or measuring highly insulating materials, if the beam current is too high, it may cause the sample to charge to potentials comparable to the incident beam energy, affecting the effective electron landing energy. Sample charging results from insufficient time for the electrons to dissipate to the underlying conductors.

Under these conditions, the beam current may be lowered and the upper detector may advantageously be used to detect secondary electrons instead of backscattered electrons as previously described. Lowering the beam current reduces surface charging, improving resolution and measurement precision in the case of highly insulated materials. By detecting secondary electrons at the upper detector, the capability to observe the bottom of high aspect ratio structures (such as trenches) is preserved under conditions such as shown in Figure 14. As can be observed from that drawing, the collection of secondary electrons at the upper detector is facilitated by applying a bias voltage of around +160v to the wafer. The face of the upper detector, instead of being negatively biased as before, is now unbiased. Secondary electrons are accelerated up the column to the upper detector, where they exhibit trajectories more similar to those of backscattered electrons.

Using upper and lower detector assemblies spaced apart in the vertical (Z-axis) direction as described, Z-axis contrast, or discrimination, may be achieved. Using other configurations of multiple detectors, both Z-axis and topographic contrast may be obtained. Whereas Z-axis contrast provides sensitivity to upper and lower surfaces, allowing the plane in which a measurement is taken to be defined, topographic contrast provides sensitivity to rising and falling edges. Referring to Figure 15A, a line 34 patterned on a substrate 33 is detected by two different detectors A and B located on opposite sides of a primary electron-optical axis. The detection waveforms detected by the respective detectors are depicted in Figure 15A above the line 34. The waveform detected by detector A exhibits a peak at the rising edge of the line (assuming a left to right scan) and, due to a shadowing effect, exhibits a valley at the falling edge of the line. The waveform detected by detector B exhibits just the opposite effect. Such signals are useful for identifying edges and determining linewidths.

Topographic contrast in two orthogonal directions may be provided using a quad detector arrangement as shown in Figure 15B. Detectors A, B, C and D occupy different quadrants of an annulus. Such a detector arrangement is commercially available from Galileo Incorporated.

In the coplanar detector arrangements of figures 15A and 15B, each of the detectors is spaced apart a substantially same scalar distance from a primary electron-optical axis. Such a configuration does not yield Z-axis contrast, as desired in order to image high-aspect-ratio structures.

Referring to Figure 16, both topographic and Z-axis contrast may be provided using an arrangement in which different detectors are spaced apart substantially different scalar distances from a primary electron-optical axis. In Figure 16, detectors A and D are spaced farther apart from the primary electron optical axis than detectors B and C. As a result, detectors A and D provide information primarily concerning the top surface of the structure being examined. These detectors are unable to effectively image high-aspect-ratio structures such as a contact hole in a layer of photoresist 35 on top of a substrate 33 as shown. Detectors B and C, because they are closer to the primary electron-optical axis, are able to image the bottom of the contact hole. The detectors of Figure 16 may be conventional Everhart-Thornley detectors or may be split-anode microchannel plate detectors.

If only Z-axis contrast is desired, a detector configuration as shown in Figure 17 may be used. Two concentric annular detectors A and B provide Z-axis contrast with detector A "seeing" deeper than detector B. The two detectors are located at the same Z level in a coplanar arrangement. This allows the detectors to be constructed as a single unit, minimizing both size and cost.

By subdividing detectors A and B in Figure 16 into quad detectors, both Z-axis and topographic contrast may be provided. The resulting configuration, shown in Figure 18, is one of two concentric annular quad detectors, quad detector A including detectors A1, A2, A3 and A4, and quad detector B including detectors B_1, B_2, B_3 and B_4. Each of the quad detectors provides topographic contrast in the same manner as the quad detector of Figure 15B. In addition, when each quad detector is taken as a unit, Z-axis contrast is obtained in the same manner as in the arrangement of Figure 17.

Using computer simulation, the locations of the different detectors of Figures 16, 17 and 18 may be optimized to achieve the most advantageous collection of electrons. Figure 19 shows a computer simulation of the trajectories of backscattered electrons through the electron microscope column of Figure 12. Electrons are assumed to travel in the -X direction so as to bombard a sample at the location of the origin (0,0). Because higher energy electrons have been found to provide better resolution than lower energy electrons, the simulation plots trajectories of elastically backscattered electrons--those electrons having the highest energy. The trajectory plot allows collection of these electrons, which come from the shallowest wafer depths and therefore resolve surface features best, to be maximized. The trajectories shown are for electrons having backscatter angles (relative to surface normal) of 0, .05, .1, . . . , 0.6 radian. In the simulation, the upper detector of Figure 12 was biased to -300V and the lower detector was set to 0V. Also shown in Figure 19 is the strength of the magnetic field produced by the magnetic lens assembly 70 of Figure 12.

Using the trajectory plot of Figure 19, the effect of different sizes and placements of annular detectors may be evaluated. For example, if two concentric annular detectors were placed at locations A and B in Figure 19, some cross-over occurs of electrons backscattered at grazing angles but subsequently reflected so as to impinge on detector B instead of detector A.

With the detectors located at positions A′ and B′, no such cross-over is experienced. With the detectors located at locations A″ and B″, a very clean differention is achieved between electrons within an inner cone of acceptance (detector B″) and electrons within an outer cone of acceptance (detector A″).

The foregoing has described the principles, preferred embodiments and modes of operation of the present invention. However, the invention should not be construed as limited to the particular embodiments discussed. Instead, the above-described embodiments should be regarded as illustrative rather than restrictive, and it should be appreciated that variations may be made in the embodiments by workers skilled in the art without departing from scope of the present invention as defined by the following claims.

WHAT IS CLAIMED:

1. Apparatus comprising:

stage means for supporting a wafer on which a microscopic structure is patterned;

means for directing a primary electron beam onto said microscopic structure; and

a plurality of detectors spaced apart substantially different scalar distances from one of

a) in the horizontal direction, a primary electron-optical axis; and

b) in the vertical direction, a wafer plane.

2. The apparatus of claim 1, having four coplanar detectors, two detectors spaced apart a first distance from said primary electron-optical axis on opposite sides thereof and two additional detectors spaced apart a second distance from said primary electron-optical axis on opposite sides thereof.

3. The apparatus of claim 1, having two coplanar, concentric, annular detectors.

4. The apparatus of claim 1, having eight detectors arranged as two coplanar, concentric, annular quad detectors.

5. The apparatus of claim 1 wherein said detectors are Everhart-Thornley detectors.

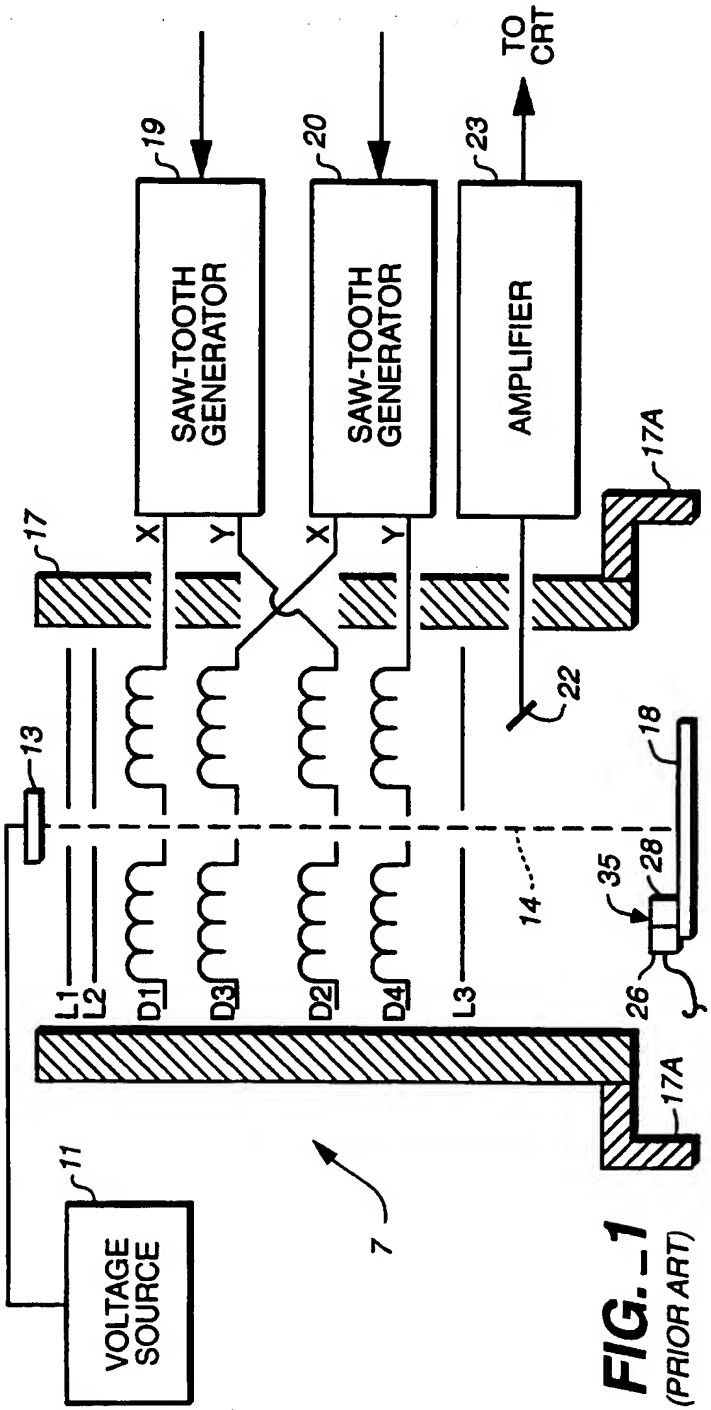

FIG._1
(PRIOR ART)

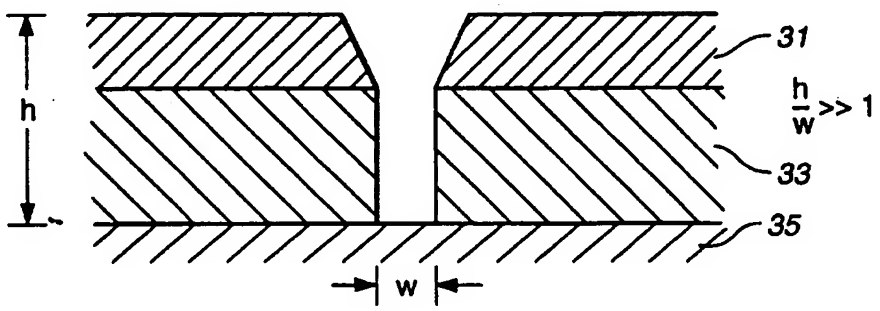

FIG._2

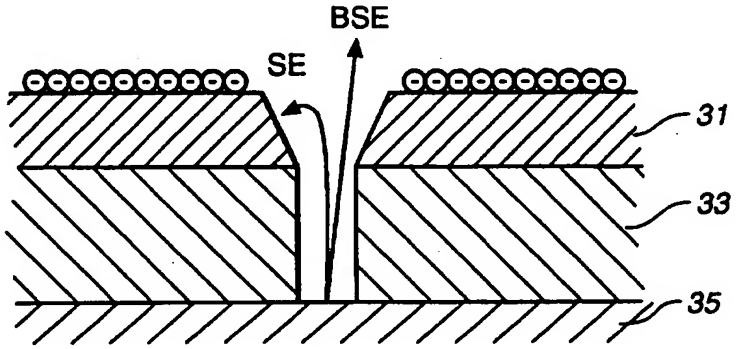

FIG._3

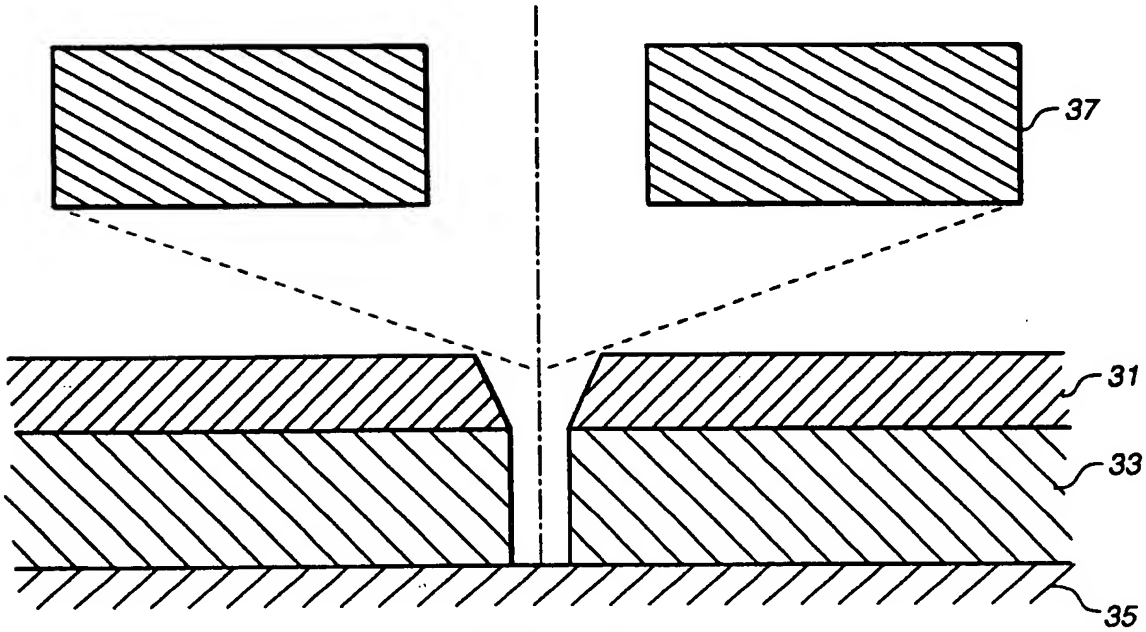

FIG._4

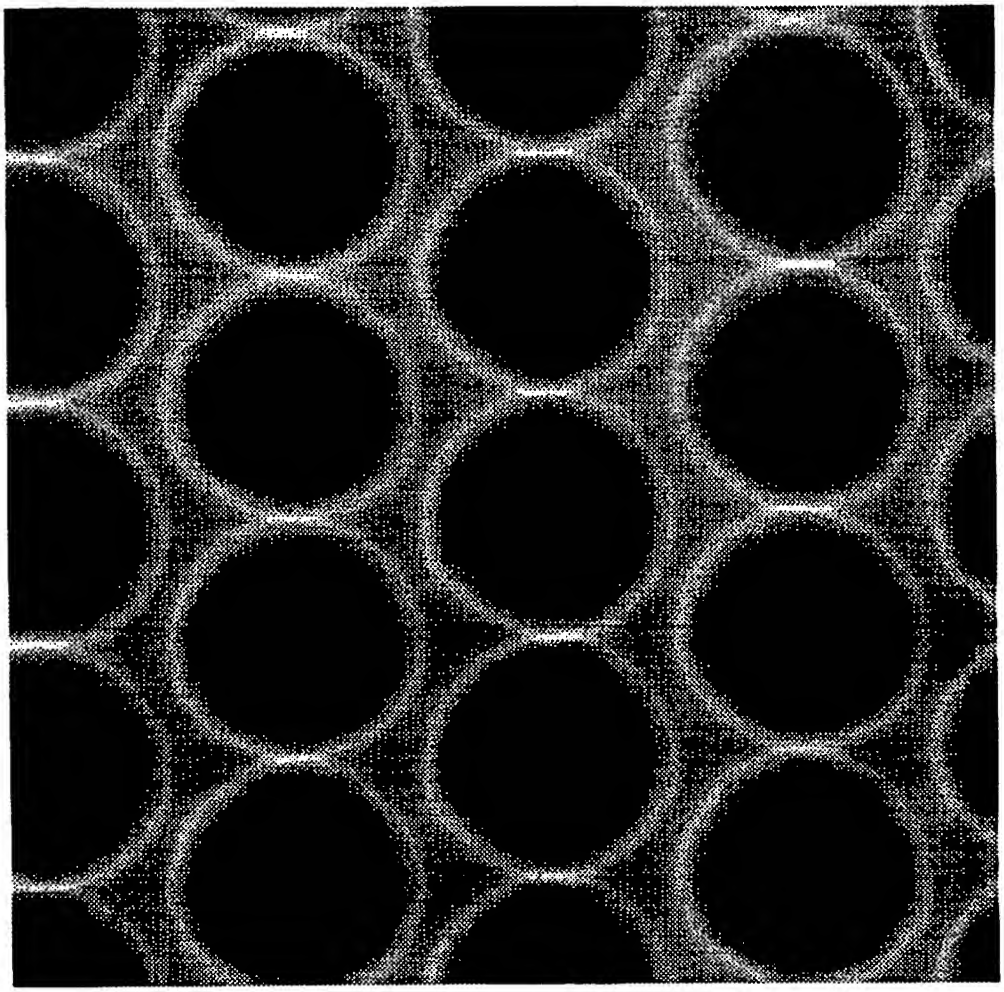

FIG._5

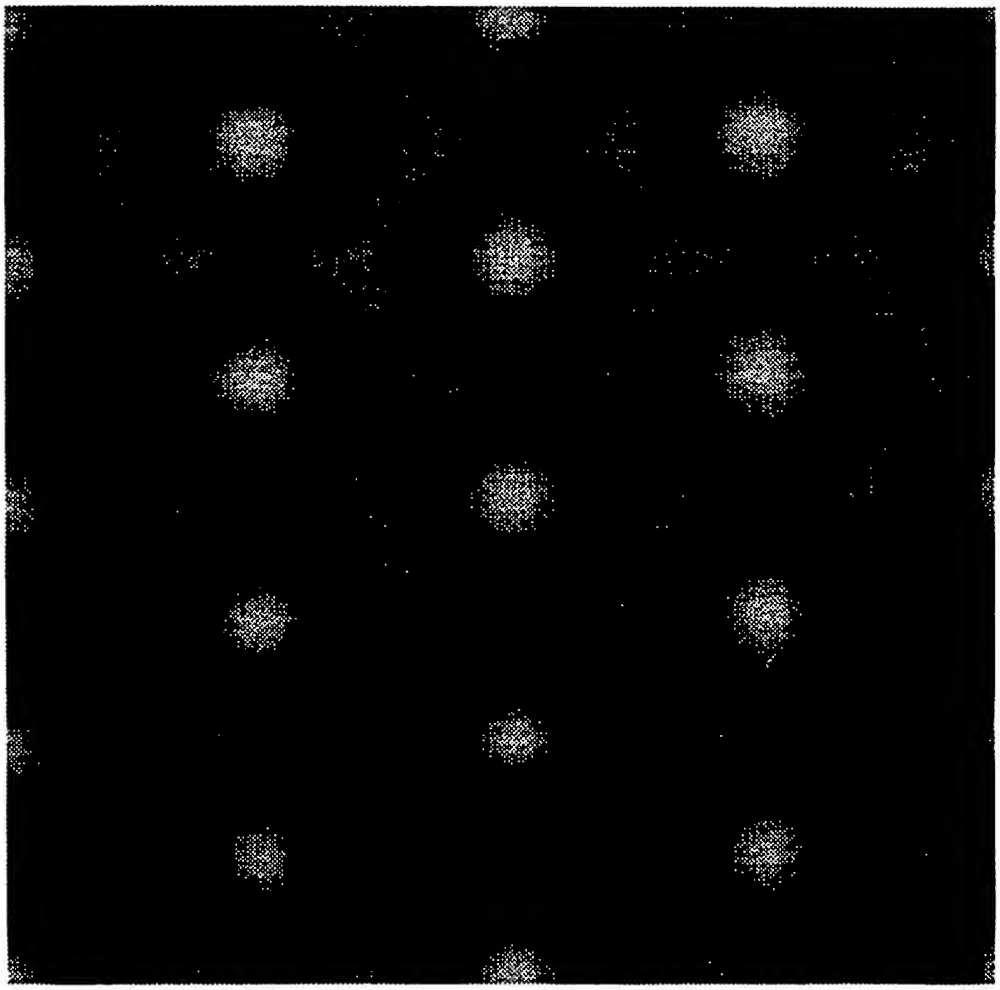

FIG._6

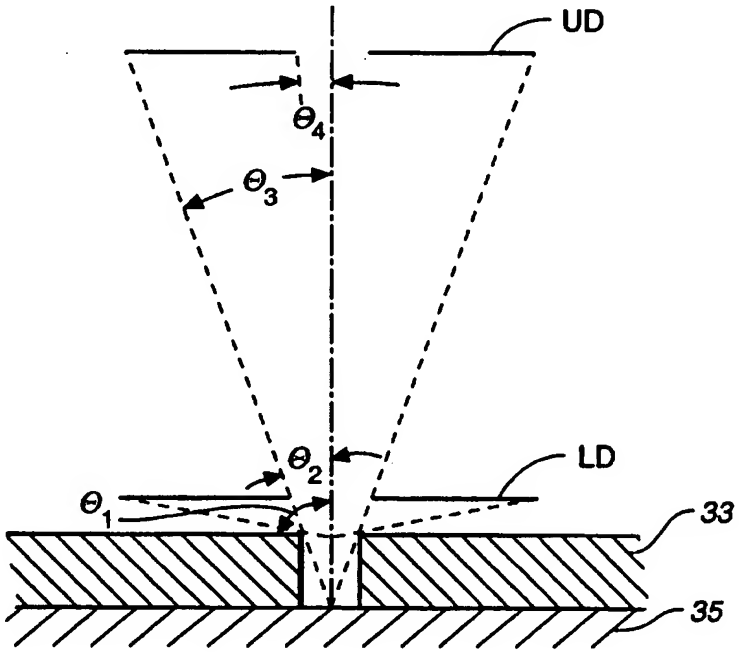

FIG._7

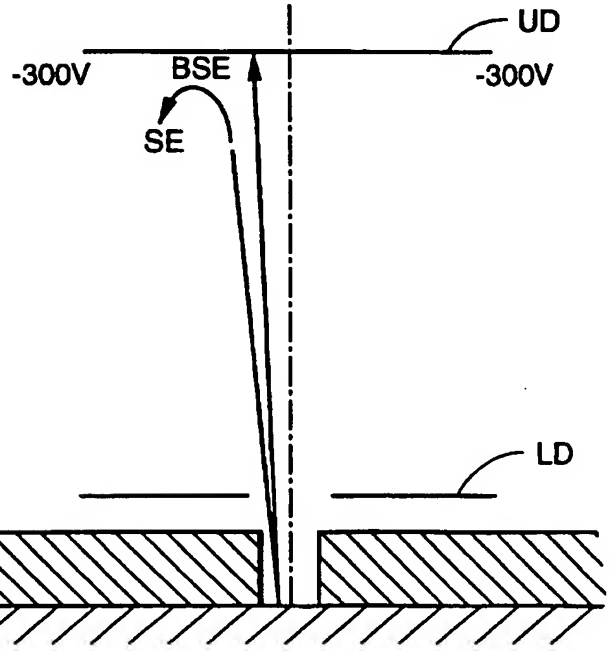

FIG._8

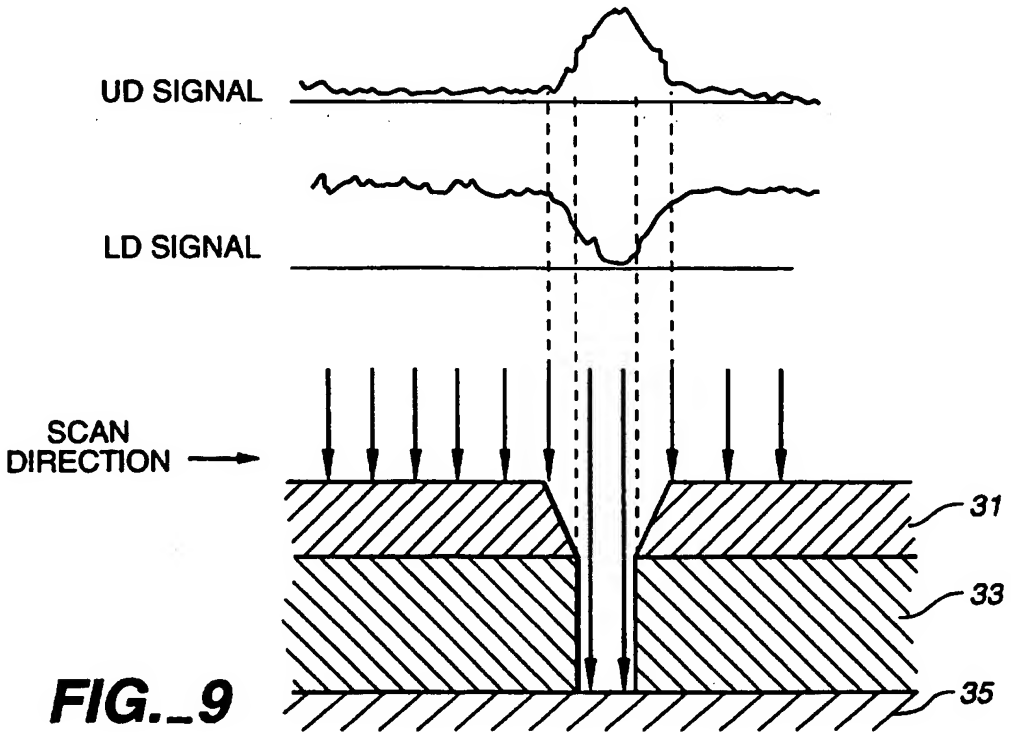
UD SIGNAL
LD SIGNAL
SCAN DIRECTION
31
33
35

FIG._9

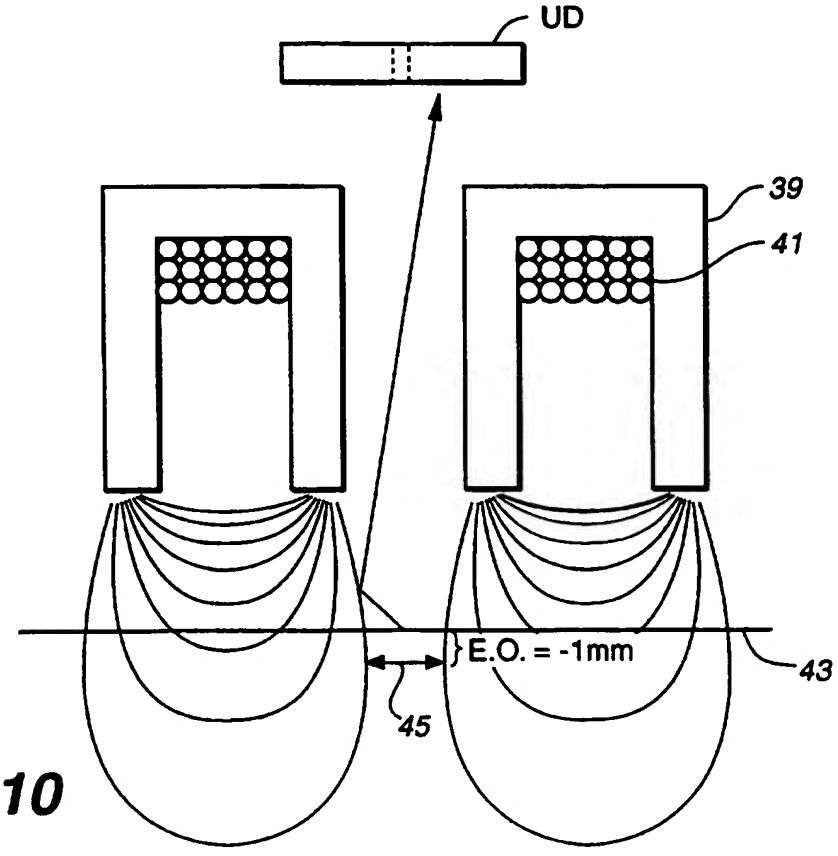
UD
39
41
E.O. = -1mm
43
45

FIG._10

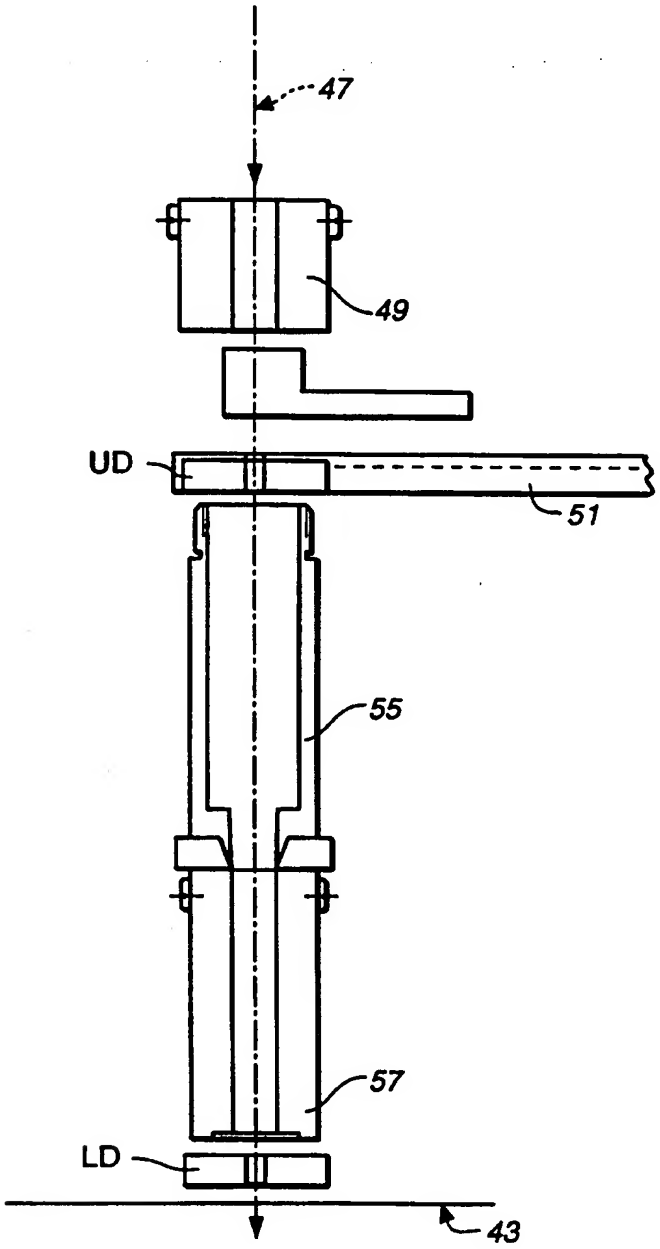

FIG._11

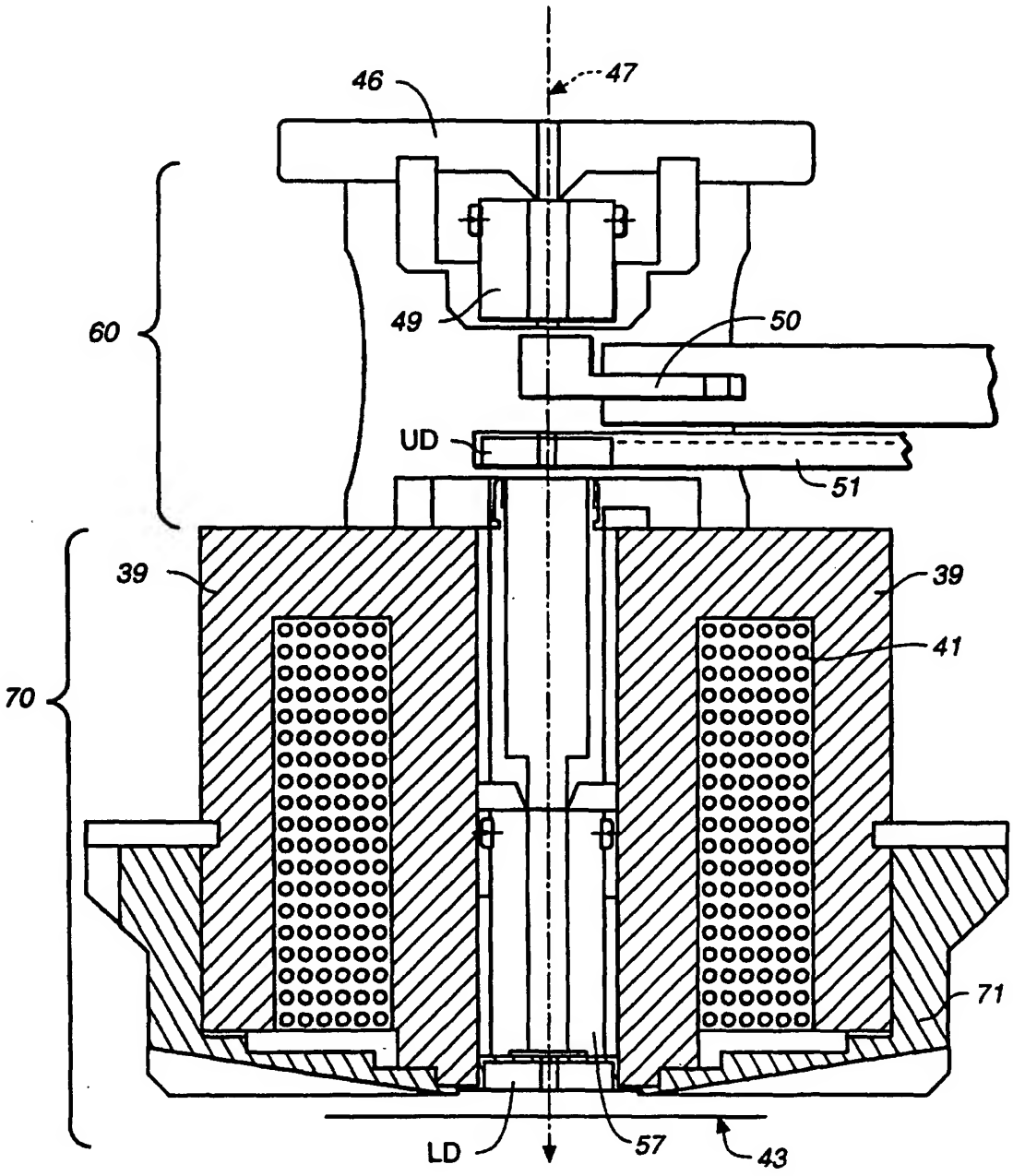

FIG._12

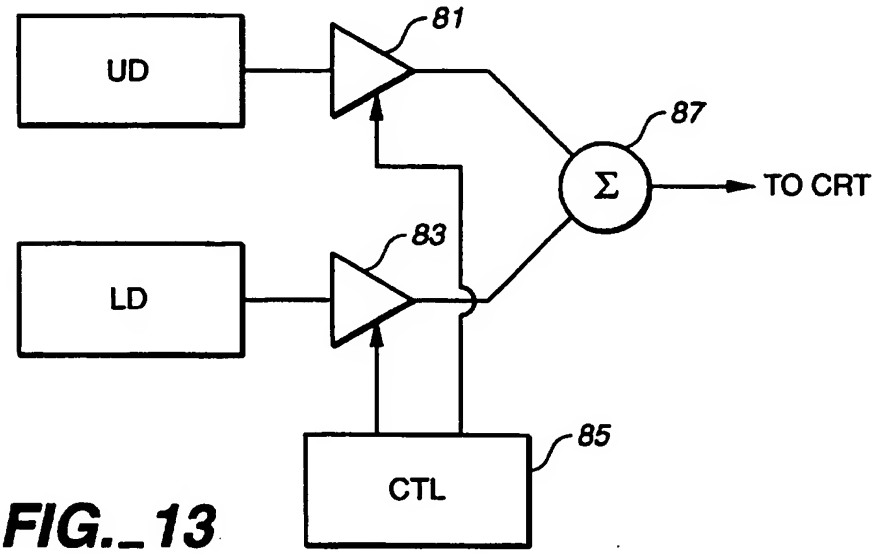

FIG._13

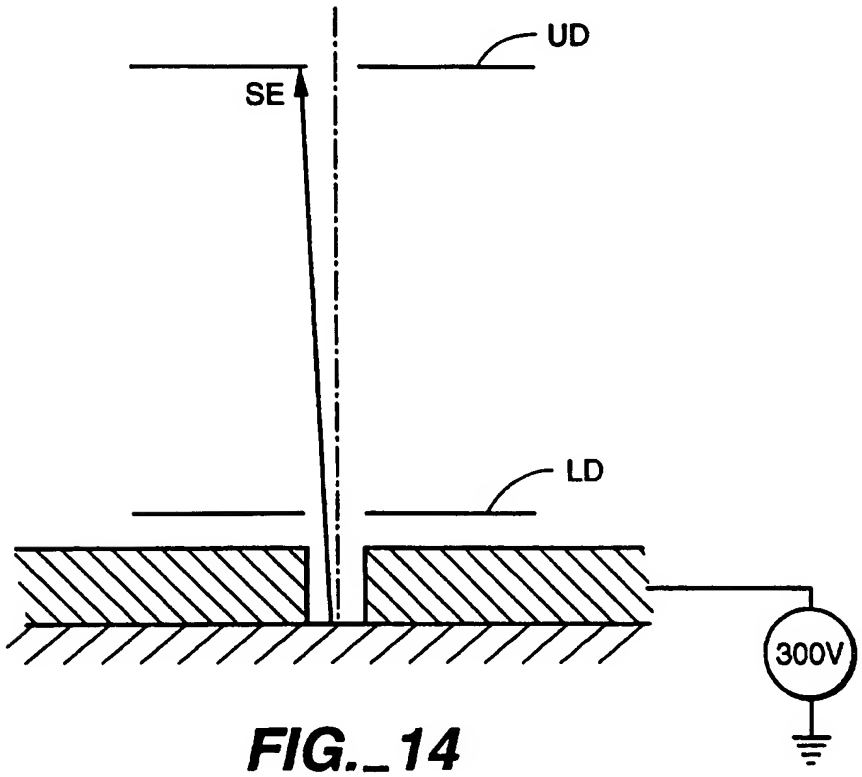

FIG._14

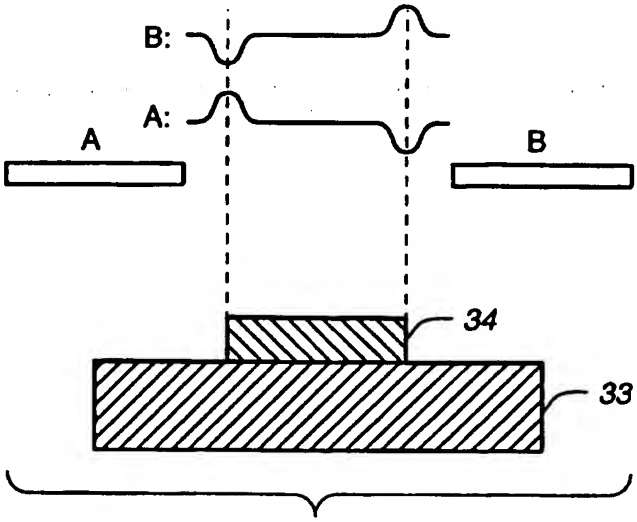

FIG._15A
(PRIOR ART)

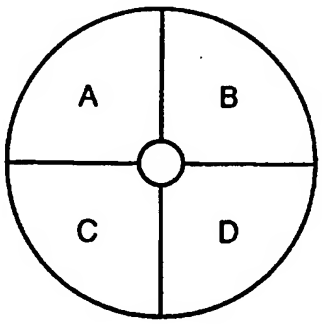

FIG._15B
(PRIOR ART)

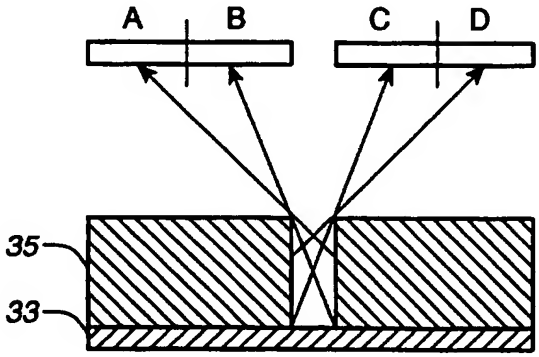

FIG._16

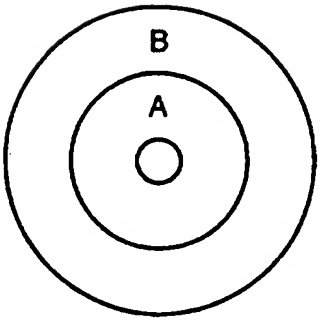

FIG._17

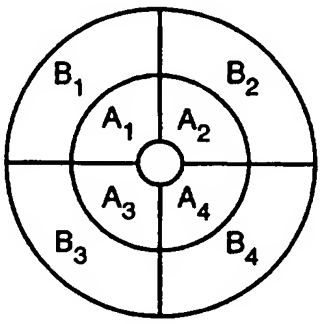

FIG._18

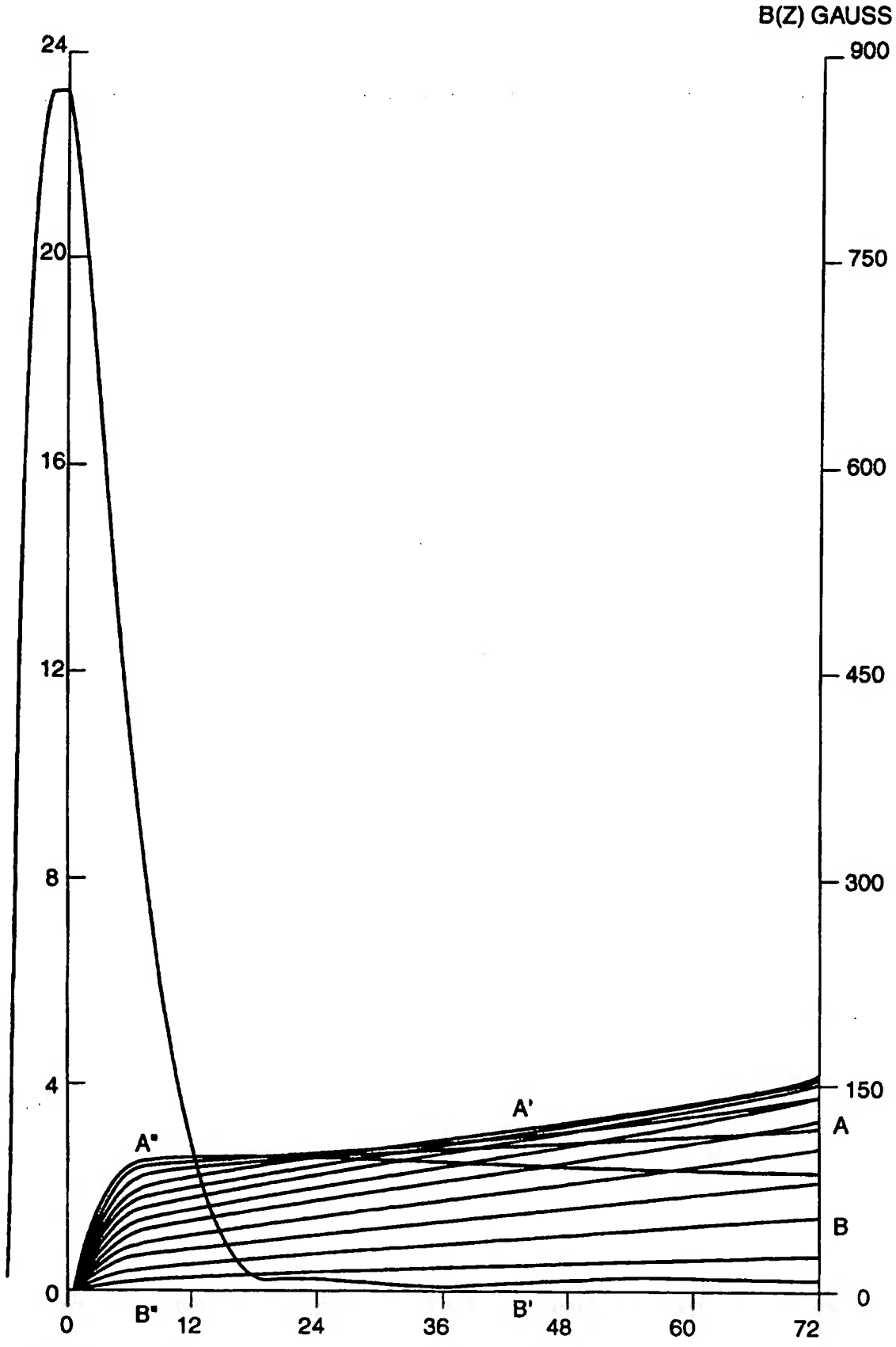
B(Z) GAUSS
24
20
16
12
8
4
0
900
750
600
450
300
150
0
A'
A"
A
B
B"
B'
0
12
24
36
48
60
72

FIG._19

INTERNATIONAL SEARCH REPORT

International application No.
PCT/US95/10566

A. CLASSIFICATION OF SUBJECT MATTER

IPC(6) :H01J 37/29,244
US CL :250,310

According to International Patent Classification (IPC) or to both national classification and IPC

B. FIELDS SEARCHED

Minimum documentation searched (classification system followed by classification symbols)

U.S. : 250/310,397,398,492.2

Documentation searched other than minimum documentation to the extent that such documents are included in the fields searched

Electronic data base consulted during the international search (name of data base and, where practicable, search terms used)

APS

C. DOCUMENTS CONSIDERED TO BE RELEVANT

Category*	Citation of document, with indication, where appropriate, of the relevant passages	Relevant to claim No.
Y	US,A 4,896,036 (ROSE ET AL) 23 JANUARY 1990. SEE CLAIM 21,LAST PARA.; COL.3, LINES 38-53; AND COL. 3, LAST PARA..	1,5
Y	US,A, 5,097,127 (HILDENBRAND ET AL) 17 MARCH 1992. SEE COL. 4, LINES 22-23 AND LINE 66- COL. 5, LINE 2; AND COL 6 FIRST PARA.	1-5
Y	US,A, 3,896,308 (VENEBLES) 22 JULY 1975. SEE ENTIRE DOCUMENT	1-5
Y	US,A, 4,896,045 (OKUNUKI ET AL) 23 JANUARY 1990. SEE COL. 3, LAST PARA.	2-4
Y	US,A, 5,198,675 (HIKITA ET AL) 30 MARCH 1993. SEE FIG. 7	2-4

☐ Further documents are listed in the continuation of Box C. ☐ See patent family annex.

*	Special categories of cited documents:	"T"	later document published after the international filing date or priority date and not in conflict with the application but cited to understand the principle or theory underlying the invention
"A"	document defining the general state of the art which is not considered to be of particular relevance	"X"	document of particular relevance; the claimed invention cannot be considered novel or cannot be considered to involve an inventive step when the document is taken alone
"E"	earlier document published on or after the international filing date	"Y"	document of particular relevance; the claimed invention cannot be considered to involve an inventive step when the document is combined with one or more other such documents, such combination being obvious to a person skilled in the art
"L"	document which may throw doubts on priority claim(s) or which is cited to establish the publication date of another citation or other special reason (as specified)	"&"	document member of the same patent family
"O"	document referring to an oral disclosure, use, exhibition or other means		
"P"	document published prior to the international filing date but later than the priority date claimed		

Date of the actual completion of the international search	Date of mailing of the international search report
26 OCTOBER 1995	14 NOV 1995
Name and mailing address of the ISA/US Commissioner of Patents and Trademarks Box PCT Washington, D.C. 20231 Facsimile No. (703) 305-3230	Authorized officer for BRUCE C. ANDERSON Telephone No. (703)308-4851

Form PCT/ISA/210 (second sheet)(July 1992)*